MOLECULAR AND CELLULAR BIOLOGY, Feb. 2007, p. 1254–1263 Vol. 27, No. 4
0270-7306/07/$08.00+0 doi:10.1128/MCB.01661-06

Interplay between Chromatin and *trans*-Acting Factors on the *IME2* Promoter upon Induction of the Gene at the Onset of Meiosis▽

Tomomi Inai,† Masashi Yukawa,† and Eiko Tsuchiya*

Department of Molecular Biotechnology, Graduate School of Advanced Sciences of Matter, Hiroshima University, Kagamiyama, Higashi-Hiroshima 739-8530, Japan

Received 6 September 2006/Returned for modification 4 October 2006/Accepted 30 November 2006

The *IME2* gene is one of the key regulators of the initiation of meiosis in budding yeast. This gene is repressed during mitosis through the repressive chromatin structure at the promoter, which is maintained by the Rpd3-Sin3 histone deacetylase (HDAC) complex. *IME2* expression in meiosis requires Gcn5/histone acetyltransferase, the transcriptional activator Ime1, and the chromatin remodeler RSC; however, the molecular basis of *IME2* activation had not been previously defined. We found that, during mitotic growth, a nucleosome masked the TATA element of *IME2*, and this positioning depended on HDAC. This chromatin structure was remodeled at meiosis by RSC that was recruited to TATA by Ime1. Stable tethering of Ime1 to the promoter required the presence of Gcn5. Interestingly, Ime1 binding to the promoter was kept at low levels during the very early stages in meiosis, even when the levels of Ime1 and histone H3 acetylation at the promoter were at their highest, making a 4- to 6-h delay of the *IME2* expression from that of *IME1*. HDAC was continuously present at the promoter regardless of the transcriptional condition of *IME2*, and deletion of *RPD3* allowed the *IME2* expression shortly after the expression of *IME1*, suggesting that HDAC plays a role in regulating the timing of *IME2* expression.

Programming the expression of the genome is essential for cell growth, differentiation, and development. The precise induction of defined sets of genes at specific stages is particularly important for cellular differentiation in eukaryotes.

Meiosis and spore morphogenesis in *Saccharomyces cerevisiae* are developmental processes of this organism. Recent microarray experiments indicated that more than 1,000 genes are induced above background levels during these processes (8, 22). The initiation of the meiotic pathway is governed by a genetic signal, indicating that the cell is diploid, and a nutritional signal, indicating that the cell is being starved by the absence of both a fermentable carbon source and nitrogen. These signals induce the expression and activation of Ime1, which serves as the master switch for meiosis (for review, see references 12, 18, and 36). Ime1 is a transcriptional activator of early meiosis-specific genes (EMGs). Of such genes *IME2*, which encodes a serine/threonine protein kinase, has particular importance; because it, together with Ime1, participates in the normal activation of EMGs (for a review, see reference 18).

A large number of EMG promoters, including that of *IME2*, contain a 9-bp site called the upstream repressor sequence (URS1), which is constitutively bound by a zinc finger protein, Ume6. When the cells are under conditions for vegetative growth, with either glucose or acetate as the sole carbon source, Ume6 interacts with Rpd3-Sin3 histone deacetylase (HDAC)- and Isw2 chromatin-remodeling complexes to repress transcription (9, 13, 14). The Isw2 complex promotes the formation of a nuclease-inaccessible chromatin structure upstream of the URS1 sequence at target genes by changing nucleosome positions, and the Rpd3-Sin3 complex deacetylates histones incorporating the URS1 site to enhance the repressed state (9). Upon activation of EMGs, Ume6 functions as an activator by tethering Ime1 to URS1 (28). This interaction between Ume6 and Ime1 requires the phosphorylation of Ime1 by Rim11 and potentially other kinases such as Mck1 (38). For the efficient activation of EMGs, Gcn5 histone acetyltransferase (HAT) and the RSC chromatin remodeling complex play pivotal roles (5, 39); and the Set3 complex, which contains a putative histone methyltransferase and two HDACs, also affects the regulation of EMGs (20). These studies indicate that the conversion of Ume6 from a repressor to an activator of EMG expression through the alteration of interacting partners and the regulation of the chromatin structure around the URS1 site by multiple chromatin remodelers are critical for the induction of EMGs and for the progression of meiosis. However, the molecular mechanisms for regulating the EMG expression in the context of chromatin are poorly understood.

Here we monitored the time course of the activation of *IME2*, focusing on the chromatin structure of the promoter region of this gene and the interplay between the factors known to be involved in the regulation.

MATERIALS AND METHODS

Strains, growth conditions, and enzyme assay. Preparation of media, genetic methods, and strain isolation followed standard procedures. Strain genotypes are shown in Table 1. All gene deletions were verified by PCR (details are available on request). *IME1*-hemagglutinin (HA) was constructed by fusing a 3xHA-epitope sequence in frame between +495C and +496G of the *IME1* open reading frame (ORF) in an integration vector, YIp5. After verification of the proper construction by sequencing, the resulted plasmid was introduced into the genomic *IME1* locus of *ime1*Δ::*TRP1* by a previously described method (27). *NPS1*-TAP was constructed by introducing a tandem affinity purification (TAP) cassette (24) in frame to the last codon of the genomic *NPS1* gene with a *kanMX* marker. Sporulation of the *IME1*-HA (WMY11-D) strain was comparable to that of the wild type (W303-1D). The *NPS1*-TAP (WHK40-D) strain grew well in YPD (1% yeast extract, 2% peptone, 2% glucose) and YPA (containing 2%

* Corresponding author. Mailing address: Department of Molecular Biotechnology, Graduate School of Advanced Sciences of Matter, Hiroshima University, Kagamiyama, Higashi-Hiroshima 739-8530, Japan. Phone and fax: 81 82 424 7868. E-mail: etsuchi@hiroshima-u.ac.jp.

† T.I. and M.Y. contributed equally to this work.

▽ Published ahead of print on 11 December 2006.

TABLE 1. Yeast strains used in this study

Strain[a]	Description	Genotype	Source or reference
W303-1D	Wild type	*MAT***a**/α homozygous for *ade2-1 leu2-3,122 his3-11,15 trp1-1 ura3-1 can1-100*	26a
WTH1-D	*nps1-105*	*nps1-105*/*nps1-105*	35
WTI20-D	*gcn5*Δ	*gcn5*Δ::*HIS3*/*gcn5*Δ::*HIS3*	This study
WMY10-D	*ime1*Δ	*ime1*Δ::*TRP1*/*ime1*Δ::*TRP1*	This study
WHS20-D	*rpd3*Δ	*rpd3*Δ::*LEU2*/*rpd3*Δ::*LEU2*	This study
WMY30-D	*sin3*Δ	*sin3*Δ::*URA3*/*sin3*Δ::*URA3*	This study
WMY40-D	*ume6*Δ	*ume6*Δ::*HIS3*/*ume6*Δ::*HIS3*	This study
WMY21-D	*rpd3*Δ *ime1*Δ	*rpd3*Δ::*LEU2*/*rpd3*Δ::*LEU2 ime1*Δ::*TRP1*/*ime1*Δ::*TRP1*	This study
WMY31-D	*sin3*Δ *ime1*Δ	*sin3*Δ::*URA3*/*sin3*Δ::*URA3 ime1*Δ::*TRP1*/*ime1*Δ::*TRP1*	This study
WHS21-D	*nps1-105 rpd3*Δ	*nps1-105*/*nps1-105 rpd3*Δ::*LEU2*/*rpd3*Δ::*LEU2*	This study
WMY31-D	*nps1-105 sin3*Δ	*nps1-105*/*nps1-105 sin3*Δ::*URA3*/*sin3*Δ::*URA3*	This study
WMY11-D	*IME1*-HA	*ime1*Δ::*TRP1*::*IME1*-HA::*URA3*/*ime1*Δ::*TRP1*::*IME1*-HA::*URA3*	This study
WMY12-D	*nps1-105 rsc2*Δ *IME1*-HA	*nps1-105*/*nps1-105 rsc2*Δ::*LEU2*/*rsc2*Δ::*LEU2 ime1*Δ::*TRP1*::*IME1*-HA::*URA3*/*ime1*Δ::*TRP1*::*IME1*-HA::*URA3*	This study
WMY13-D	*gcn5*Δ *IME1*-HA	g*cn5*Δ::*HIS3*/*gcn5*Δ::*HIS3 ime1*Δ::*TRP1*::*IME1*-HA::*URA3*/*ime1*Δ::*TRP1*::*IME1*-HA::*URA3*	This study
WHK40-D	*NPS1*-TAP	*NPS1*-TAP::*kanMX*/*NPS1*-TAP::*kanMX*	This study
WMY14-D	*ime1*Δ *NPS1*-TAP	*ime1*Δ::*TRP1*/*ime1*Δ::*TRP1 NPS1*-TAP::*kanMX*/*NPS1*-TAP::*kanMX*	This study
WMY15-D	*IME1*-HA *NPS1*-TAP	*ime1*Δ::*TRP1*::*IME1*-HA::*URA3*/*ime1*Δ::*TRP1*::*IME1*-HA::*URA3 NPS1*-TAP::*kanMX*/*NPS1*-TAP::*kanMX*	This study

[a] All strains are derivatives of the W303 genetic background.

potassium acetate instead of the glucose in YPD), showed no detectable growth defect, and sporulated equivalently to the wild type.

Yeast cells were vegetatively grown in YPD at 28°C. To induce sporulation, cells were grown in YPA for at least 3 generations at 28°C and harvested at 2×10^7 to 4×10^7 cells/ml. The cells were washed twice with sporulation medium (SPM; 1% potassium acetate) and then resuspended at 1.5×10^7 cells/ml in the same medium.

β-Galactosidase activity was assayed by using permeabilized cells carrying pMY264 (*IME2p*::*lacZ URA3*), as described previously (39).

Chromatin structure analysis. Digestion of chromatin with micrococcal nuclease (MNase) and Southern blotting were done essentially as described previously (35), except that spheroplasting of the cells was done by incubation with Zymolyase at 37°C for 10 min (Seikagaku Corporation). BstEII was used to digest the deproteinized DNA samples after purification. The experiment was performed at least three times, and typical results are presented.

Northern and Western blot analyses. RNA preparation, Northern blotting, preparation of protein samples, and Western blotting were carried out as described earlier (15, 39). The intensity of the mRNA bands obtained by Northern blotting was measured by using a BAS-2000 Bioimaging analyzer (Fuji Photo Film Co.), and mRNA levels were normalized to the individual U3 RNA level.

ChIP. Chromatin immunoprecipitation (ChIP) analysis was done essentially as described (11) with the following modifications: antibody-treated fractions (400 μl) were incubated with 15 μl of Dynabeads-protein G (Dynal Biotech) at 4°C for 3 h with gentle rotation. For precipitation using TAP-tagged proteins, 10 μl of immunoglobulin G (IgG)-Sepharose (Amersham Bioscience) was used in 400 μl of sheared chromatin. The bead-bound immune complexes were washed twice with 1.0 ml of lysis buffer (50 mM HEPES-KOH, pH 7.5, containing 140 mM NaCl, 1% Triton X-100, 0.1% sodium deoxychorate, 0.1% sodium dodecyl sulfate, 1 mM EDTA), 1.0 ml of high-salt lysis buffer (50 mM HEPES-KOH, pH 7.5, containing 500 mM NaCl, 1% Triton X-100, 0.1% sodium deoxycholate, 1 mM EDTA), and 1.0 ml of wash buffer (10 mM Tris-HCl, pH 8.0, containing 250 mM LiCl, 0.5% NP-40, 0.5% sodium deoxycholate) and once with 1.0 ml of TE (10 mM Tris-HCl, pH 8.0, containing 1 mM EDTA). Quantitative PCR was performed on undiluted immunoprecipitated-DNA samples or 50- to 100-fold-diluted input chromatin samples. The linear range of template for multiplex PCR was determined empirically. Each experiment was repeated at the chromatin immunoprecipitation and PCR steps. The following antibodies were used: anti-histone H3 C terminus (Abcam), anti-histone H3 acetyl K9/14 (Upstate), anti-yeast Rpd3 (Upstate), anti-yeast Gcn5 (Santa Cruz Biotechnology), and anti-HA (BAbCO). The PCR primers amplified the following regions, whose coordinates are given relative to ATG (+1). *IME2* URS1 primers amplified the 352-bp region from −712 to −361, *IME2* TATA primers amplified the 294-bp region from −330 to −37, *IME2* ORF primers amplified the 350-bp region from +40 to +389, *SPO13* URS1 primers amplified the 413-bp region from −320 to + 93, *LEU2* ORF primers amplified the 244-bp region from +227 to +470; *HTA1* ORF primers amplified the 245-bp region from −25 to +220, *HTA1*/*HTB1* promoter primers amplified the 301-bp region from −360 to −660, and Chr-VI TEL primers amplified the 293-bp region from 269,352 to 269,644 of chromosome VI.

TAP. The extraction of yeast cells and TAP were performed as described previously (33). Purified proteins were concentrated by lyophilization and subjected to immunoblotting.

RESULTS

Nucleosome positioning and remodeling at the *IME2* promoter. To understand the chromatin structure around the promoter region of the *IME2* gene, we performed nucleosome mapping on the wild-type cells grown vegetatively in rich medium (YPD) by using micrococcal nuclease (MNase) digestion followed by restriction enzyme (BstEII) cutting and Southern blotting (Fig. 1A, lane Y). MNase preferentially digested the chromatin at approximately nucleotides (nt) +140, −20, −180, −330, −470, and −620 of the *IME2* ORF. This result indicates that six nucleosomes are positioned in an ordered array between the two BstEII sites, corresponding to nt −747 and +249 of the *IME2* ORF, and two TATA sequences (nt −121 to ~−126 and −163 to ~−168) were masked by nucleosome −1, as schematically shown in Fig. 1A. The *IME2* promoter contains two URS1 sequences: one at nt −449 to ~−457 and the other at −544 to ~−552. These two sites were located at nucleosomes −3 and −4, respectively. After the cells had been grown in rich medium containing acetate as the sole carbon source, alteration of the MNase sensitivity at several sites was detectable; however, few novel cutting bands appeared, indicating that the positioning of nucleosomes was not altered under this growth condition (YPA, Fig. 1A, SPM, 0 h, wild type).

When the wild-type cells were incubated in SPM for 2 h, faint cutting bands appeared within the regions indicated to be occupied by nucleosomes −1 and −2 (Fig. 1A, shown by the closed triangles). The intensity of these bands gradually in-

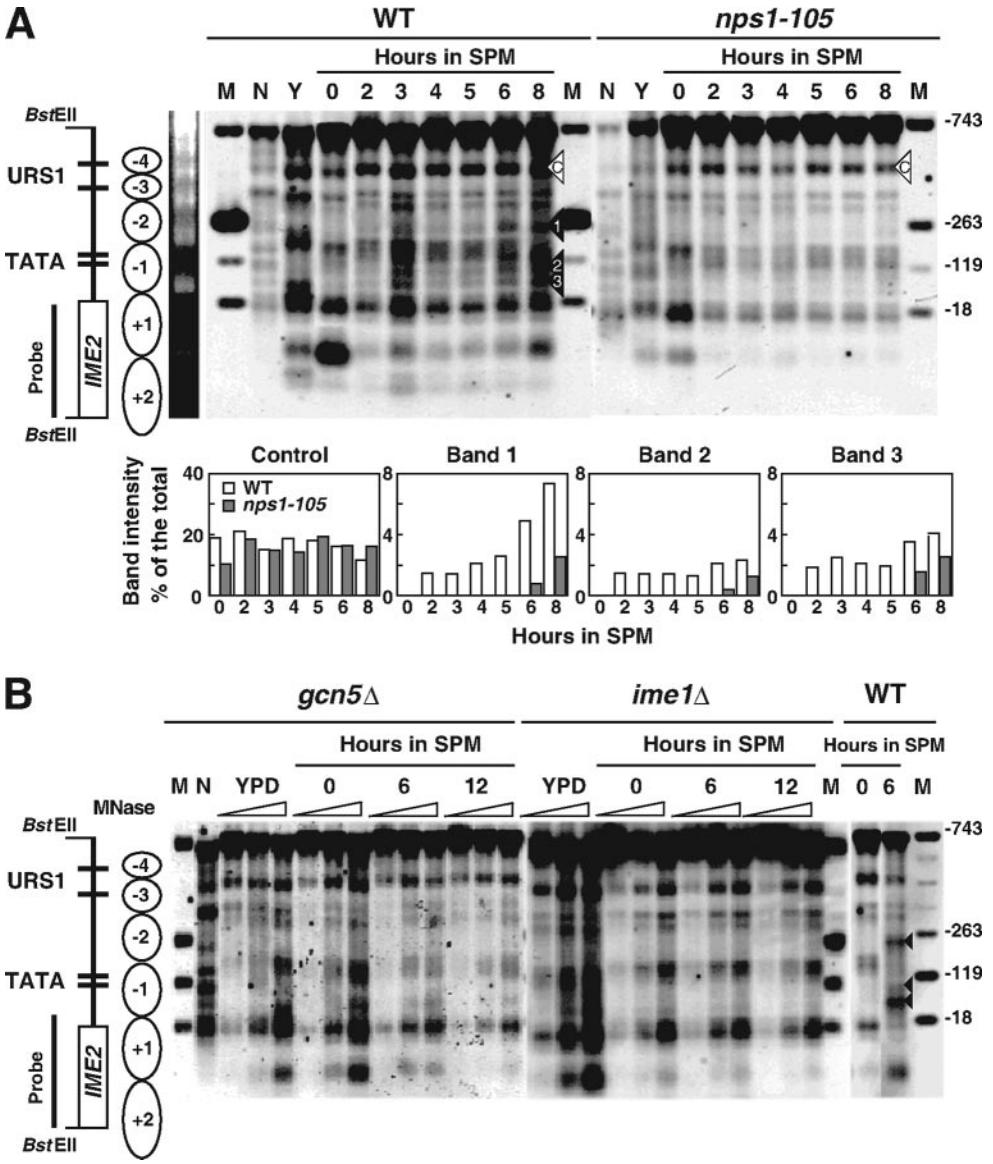

FIG. 1. Analysis of chromatin structure of the *IME2* gene. (A) Wild type (WT; W303-1D) or *nps1-105* (WTH1-D) cells were harvested at the indicated times and processed for MNase digestion. Positions of nucleosomes with respect to the *IME2* sequence are schematically indicated on the left side of the figure. MNase cleavage sites enhanced or not enhanced (control) in the wild type are marked with closed or open triangles, respectively. Southern blots were scanned by a Bioimaging analyzer, and the percentage of the newly appeared bands in SPM, relative to all bands produced in the same lane was calculated (bar graphs below the panel). N, the naked DNA control; Y, the sample from cells vegetatively growing in YPD medium. From the top, the sizes of the marker bands are 992, 512, 368, and 267 bp. The nucleotide positions of the *IME2* ORF corresponding to each marker band are indicated on the right side. This experiment was performed three times with good consistency. Typical results are presented. (B) MNase mapping was carried out on *gcn5*Δ (WTI20-D) or *ime1*Δ (WMY10-D) cells as described for panel A.

creased toward 8 h, albeit the increase in band 2 was subtle. The kinetics of the appearance and increase in the density of these cutting bands showed a good correlation with the initiation of and increase in the synthesis of *IME2* mRNA (Fig. 1A and see Fig. 5B), indicating that the chromatin structure around the TATA box had been altered upon the shift to SPM to initiate gene expression.

We previously showed that *nps1-105*, a temperature-sensitive mutant allele of the *STH1/NPS1* gene, which encodes the ATPase subunit of the RSC chromatin-remodeling complex, caused a notable delay and decrease in *IME2* expression at 28°C, the permissive temperature of the mutation, as well as poor sporulation (39, 40) (Fig. 5B). In order to examine whether this alteration of the chromatin structure depended on Nps1/RSC, we performed nucleosome mapping on the *nps1-105* homodiploid strain. Although the MNase cutting pattern of the vegetatively growing mutant cells was similar to that of the wild type, the appearance of additional cutting bands at the region of nucleosomes −1 and −2 in SPM was notably delayed in the mutant; i.e., they appeared by 6 h after the shifting of the mutant to SPM, whereas they appeared by 2 h in the case of wild-type cells. The delayed alteration of the chromatin struc-

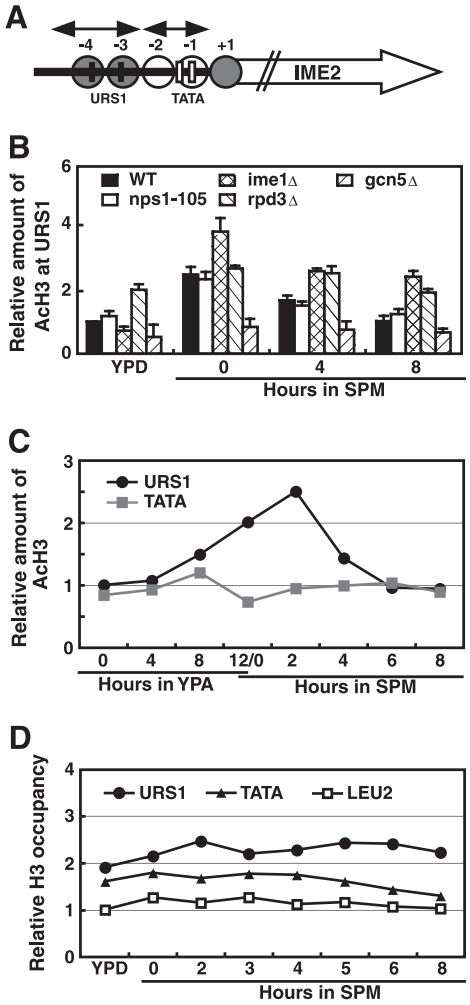

FIG. 2. Histone H3 modification at the *IME2* promoter. (A) A schematic model for the chromatin structure at the *IME2* promoter. Positions of the PCR fragments used for ChIP analysis are shown with respect to the nucleosomal organization of the repressed promoter (Fig. 1). Nucleosomes remodeled at the active promoter are indicated by open circles. URS1 (black box) and the TATA box (open box) are also indicated. (B) ChIP analysis of acetylated histone H3 levels over the *IME2* URS1. DNA was immunoprecipitated with anti-acetylated histone H3 from wild type (WT; W303-1D), *nps1-105* (WTH1-D), *gcn5*Δ (WTI20-D), *ime1*Δ (WMY10-D), and *rpd3*Δ (WHS20-D) cells. The amount of immunoprecipitated DNA was determined by PCR with primer pairs directed against *IME2*-URS1. As a control, a primer set was also used for a region 0.5 kb from the telomere of chromosome VI-R (TEL). The relative amount of acetylated histone H3 was determined as the ratio of immunoprecipitated URS1 product relative to the TEL product divided by the ratio of the respective input product. The values are shown with the amount of vegetatively growing (YPD) wild-type cells given as 1. The values shown are averages of three independent experiments. (C) Time course of histone H3-acetylation in the wild-type strain. The amount of immunoprecipitated DNA was determined by PCR and calculated as described for panel B and is shown as a relative amount with the value of the URS1 of YPD-grown cells (0 h of YPA) referred to as 1. The values are averages of four independent experiments. The standard deviation was within ±0.3. (D) ChIP analysis of histone H3 levels over the *IME2* promoter. The amount of DNA coimmunoprecipitated with anti-histone H3 carboxy terminus was determined by PCR with primer pairs directed against the *IME2*-URS1 and TATA regions. As a control, the primer set was also used for *LEU2*. Relative histone occupancy was determined as the ratio of immunoprecipitated URS1 and TATA products relative to the *LEU2* product of YPD-grown cells given as 1, after normalization with the ratio of input products. The value at each time point is an average of three independent experiments. The standard deviation was within ±0.3 for LEU2 and TATA and ±0.5 for URS1.

ture in the *nps1-105* strain is in good agreement with the delay of *IME2* expression in this strain (Fig. 5B), indicating that Nps1/RSC played a role in this alteration.

For initiation of *IME2* expression, the Ime1 transcription activator and Gcn5 HAT play pivotal roles (5, 18). So, we examined the involvement of these two factors in the chromatin structure at the *IME2* promoter. In the absence of either gene, there was no MNase hypersensitivity of either the region of nucleosomes −1 and −2 or other regions after a longer incubation period (12 h) in SPM (Fig. 1B). Taken together, the data indicate that at the onset of meiosis, Gcn5/HAT, Ime1, and RSC functioned to alter the chromatin structure around the TATA box of *IME2*. As the loss of Gcn5 or Ime1 or mutations of RSC components abrogated or delayed the *IME2* expression, this chromatin remodeling would appear to be essential for the gene activation.

Enrichment of acetylated histone H3 transiently occurs at URS1. The recruitment of one coactivator may stimulate the recruitment of another, and this interdependence can be reflected in a sequential order of coactivator recruitment to the promoter. We wanted to know the order of recruitment of Gcn5/HAT, Ime1, and RSC to the *IME2* promoter; and so we first assessed the kinetics of histone H3 acetylation at the URS1 site during the course of *IME2* activation. To examine this issue, we carried out ChIP analysis by using anti-acetylated histone H3 antibody. In this experiment, we used primers for a region 0.5 kb from the telomere of chromosome VI-R (269,352 to ~29,644), a site that is not transcribed (29), as an internal normalization control for each PCR. After quantification of each PCR product, values were normalized with the control value and are shown in Fig. 2B, with the amount of vegetatively-growing (YPD) wild-type cells taken as 1. The increase in H3 acetylation was transient, and, interestingly, the highest level of acetylation was observed at the time of the shift to SPM when the locus is in a transcriptionally inactive state. As reported earlier (5), the increase in acetylation levels was dependent upon Gcn5 and the acetylation level was constitutively high when Rpd3 was absent. The kinetics of H3 acetylation observed with both *nps1-105* and *ime1*Δ was similar to that of the wild type, indicating that the increase in H3 acetylation depended upon neither RSC nor Ime1. We also assessed histone H4 acetylation; however, little increase was detectable (data not shown) as described earlier (5).

As was shown in Fig. 1A, the introduction of MNase hypersensitivity occurred for the nucleosomes that occupied the TATA box and 5′ flanking sequences. These results suggest a possibility that the acetylation of histone H3 within these nucleosomes would increase upon shifting of the cells to meiotic conditions. Because the results of Fig. 2B suggested that the increase in histone H3 acetylation at the URS1 site was initiated during the period when the cells were growing in YPA, we monitored the H3 acetylation at the TATA box and the URS1 site during the incubation in YPA and after the shift to SPM.

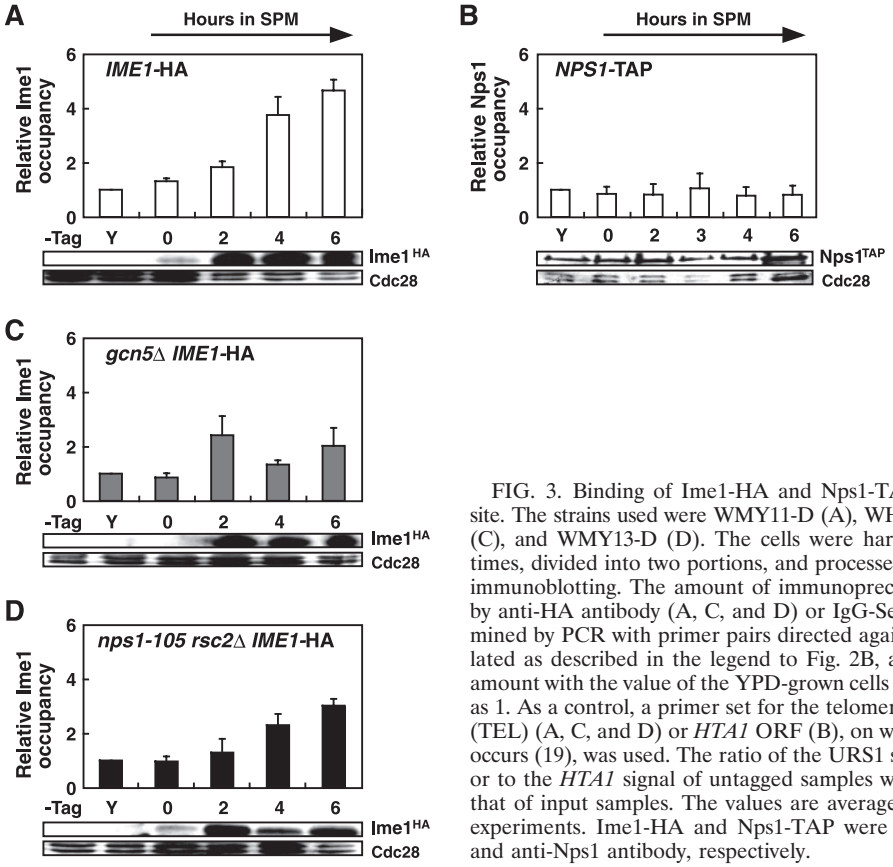

FIG. 3. Binding of Ime1-HA and Nps1-TAP to the *IME2* URS1 site. The strains used were WMY11-D (A), WHK40-D (B), WMY12-D (C), and WMY13-D (D). The cells were harvested at the indicated times, divided into two portions, and processed for ChIP analysis and immunoblotting. The amount of immunoprecipitated DNA obtained by anti-HA antibody (A, C, and D) or IgG-Sepharose (B) was determined by PCR with primer pairs directed against *IME2*-URS1, calculated as described in the legend to Fig. 2B, and shown as a relative amount with the value of the YPD-grown cells (Y) of each strain taken as 1. As a control, a primer set for the telomere of chromosome VI-R (TEL) (A, C, and D) or *HTA1* ORF (B), on which no binding of RSC occurs (19), was used. The ratio of the URS1 signal to the TEL signal or to the *HTA1* signal of untagged samples was almost equivalent to that of input samples. The values are averages of three independent experiments. Ime1-HA and Nps1-TAP were detected with anti-HA and anti-Nps1 antibody, respectively.

The level of H3 acetylation at URS1 increased after a 4-h incubation in YPA, peaked at 2 h after the shift to SPM, and then declined (Fig. 2C). On the other hand, the H3 acetylation level at the TATA box was almost constant throughout the course of the experiment. Recent studies showed that nucleosomes are lost at the promoter of the budding yeast *PHO5* gene during transcriptional induction (3, 23). Thus, we wanted to know whether the low H3 acetylation level at the TATA box reflected nucleosome loss. For this purpose, we carried out a ChIP analysis using an antibody against the C terminus of histone H3 that had been used in an earlier study establishing that nucleosomes are removed from the *PHO5* promoter (23). As an internal normalization control, we included primers for the *LEU2* gene, the transcriptional level of which is little affected by the induction of meiosis (8, 16). Figure 2D shows that the relative amount of PCR products corresponding to the URS1 and TATA regions changed little during the 8-h incubation in SPM, indicating that the low level of H3 acetylation at TATA was not due to the absence of nucleosomes. We also assessed the binding of Gcn5 to URS1 by ChIP analysis by using anti-Gcn5 antibody; however, the amount of URS1 DNA that coimmunoprecipitated with anti-Gcn5 antibody was near background levels at all time points tested (data not shown).

Gcn5 is required for sustained binding of Ime1. Figure 2 shows that the enrichment of H3 acetylation at the *IME2* promoter occurred at the URS1 site. Despite the fact that H3 acetylation occurred in the *ime1*Δ or *nps1-105* strain, alteration of the chromatin structure monitored by MNase digestion was not detectable when these strains were incubated in SPM (Fig. 1), suggesting a possibility that this histone modification functioned for recruitment of Ime1, RSC, or both. In order to determine the timing of Ime1 and RSC recruitment to the *IME2* promoter, we constructed a strain expressing HA-tagged Ime1 (*IME1*-HA) and one expressing TAP-tagged Nps1 (*NPS1*-TAP) from the genomic *IME1* and *NPS1* loci, respectively, and carried out ChIP analysis using an antibody against HA epitope or IgG-Sepharose for the respective strains. Expression of each protein was monitored by immunoblotting. Both constructs suppressed the phenotypes of the mutation of the respective genes (sporulation defect of *ime1*Δ and lethality of *nps1*Δ) and allowed the cells to sporulate with an efficiency equivalent to that of the wild type, showing that they were functional. Figure 3A shows that a small amount of Ime1-HA was expressed at the time of the shift of the wild type to SPM. The protein levels rapidly increased by 2 h, and then they were constantly maintained until 6 h. Ime1-HA occupancy at the *IME2* URS1 site was detectable after 2 h in SPM, and its level rapidly increased by 4 h. This kinetics of Ime1 binding is in good agreement with that of *IME2* expression (Fig. 5B); however, the binding was in a notable delay when compared with the kinetics of the protein accumulation. On the other hand, the protein level of Nps1-TAP was almost constant during the incubation in SPM, and Nps1-TAP binding at the URS1 site was near the background level at all time points tested (Fig. 3B): i.e., the ratio of the PCR product of immunoprecipitated URS1 relative to that of the internal control, *HTA1* ORF, on which no binding of RSC was detected by a

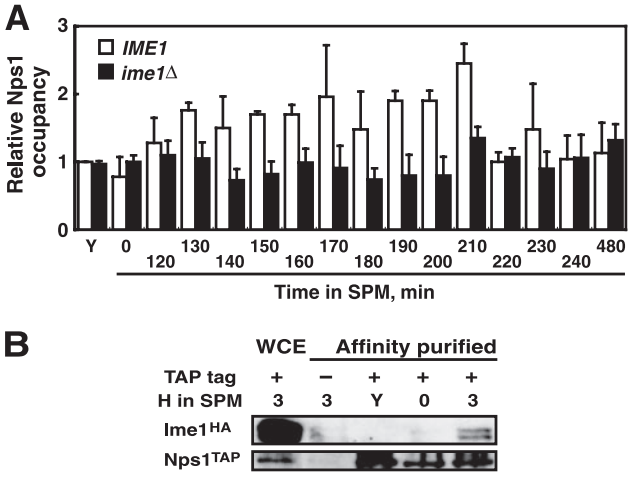

FIG. 4. Nps1/RSC transiently binds to the *IME2* TATA box. (A) Time course of Nps1-TAP binding to the *IME2* TATA sequence. The strains used were WHK40-D (*IME1*) and WMY14-D (*ime1*Δ). The amount of immunoprecipitated DNA was determined by PCR with primer pairs directed against the *IME2* TATA, calculated as described in the legend to Fig. 2B and shown as a relative amount referring to the value of the YPD-grown cells (Y) of *IME1* as 1. As a control, a primer set for *HTA1* ORF was used. The ratio of the TATA signal to the *HTA1* signal of untagged samples was almost equivalent to that of input samples. The values are averages of three independent experiments. (B) Ime1-HA is copurified with Nps1-TAP. The *NPS1*-TAP *IME1*-HA (WMY15-D) or *NPS1 IME1*-HA (minus TAP tag; WMY11-D) cells were harvested at the indicated times and processed for TAP. Proteins eluted from a calmodulin-Sepharose gel were concentrated by lyophilization and then immunoblotted with anti-HA and anti-Nps1 antibodies.

genome-wide location analysis and ChIP (19) did not exceed the ratio obtained with untagged sample (data not shown). We verified the binding of Nps1-TAP at the regulatory region of the *HTA1/HTB1* promoter in vegetatively growing cells, as reported by Ng et al. (19), showing that the lack of binding of Nps1-TAP to URS1 was not due to the impairment of IP.

Next, we asked whether the binding of Ime1-HA to URS1 required the function of Gcn5. ChIP analysis carried out on the *gcn5*Δ *IME1*-HA strain revealed that Ime1 occupancy at URS1 did not stably increase in this strain when the cells were shifted to meiotic conditions (Fig. 3C). This result indicates that the presence of Gcn5 was required for the stable binding of Ime1. The levels of Ime1-HA expression and the kinetics of its accumulation in *gcn5*Δ *IME1*-HA were almost equivalent to those for the isogenic *GCN5 IME1*-HA strain.

RSC interacts with Ime1 and transiently binds to TATA. As suggested from the data in Fig. 1, if RSC remodeled nucleosomes −1 and −2, it might make contact with these nucleosomes. To examine this issue, we carried out ChIP on *NPS1*-TAP for enrichment of TATA sequence in the precipitates. First, we carried out ChIP analysis on the cells withdrawn from the culture at 1-h intervals during the 6-h incubation in SPM. In the 3-h samples, a level of TATA sequence 1.6 times higher than that for vegetative cells was recovered. Then we examined the binding at 10-min intervals during the course of 120 to 240 min of incubation in SPM (Fig. 4A). Significant, albeit modest, enrichment of the TATA sequence was observed between 130 and 210 min, showing that Nps1-TAP transiently bound to TATA.

As was shown in Fig. 3A, Ime1 binding to URS1 was initiated after a 2-h incubation in SPM with virtually the same timing as that of RSC. This finding suggests the possibility that Ime1 recruited RSC or vice versa. In order to examine this possibility, we constructed *nps1-105 rsc2*Δ *IME1*-HA and *ime1*Δ *NPS1*-TAP strains and performed ChIP analysis using anti-HA antibody and IgG-Sepharose, respectively. Although *nps1-105 rsc2*Δ *IME1*-HA showed severe defects in *IME2* expression and sporulation (less than 5% after a 96-h incubation in SPM), both the expression level of Ime1-HA and its occupancy at URS1 occurred with kinetics similar to those observed for the wild type (Fig. 3D) (data for *IME2* expression of *nps1-105 rsc2*Δ *IME1*-HA not shown). On the contrary, Nps1-TAP occupancy at TATA was greatly reduced by the *IME1* deletion (Fig. 4A). These observations indicate that Ime1 was required for the recruitment of RSC. To assess whether Ime1 physically interacted with the RSC complex, we carried out the TAP of RSC and asked whether Ime1 would be copurified with the complex. As shown in Fig. 4B, Ime1 was detectable in the affinity-purified sample from the cells of incubated for 3 h in SPM, but was not detectable in the nontagged preparation, indicating that Ime1 physically interacted with the RSC complex.

In the absence of the Rpd3-Sin3 complex, *IME2* is expressed with earlier timing and RSC is dispensable for transcriptional activation. Our results described above show that the recruitment of Ime1 and RSC to the *IME2* promoter and the remodeling of nucleosomes at −1 and −2 were initiated with almost the same timing: i.e., 2 h after shifting the wild-type cells to SPM. These results indicate that the binding of Ime1 to the URS1 site is a rate-limiting step for this chromatin remodeling and the subsequent activation of *IME2* transcription. Our results also suggest that the Ime1 binding to URS1 required Gcn5, which was responsible for the acetylation of histone H3 at URS1. Intriguingly, the amount of the binding of Ime1 to URS1 at 2 h in SPM was quite small, in spite of the fact that both the level of H3 acetylation at URS1 and the amount of Ime1 expression were at their highest at this time point (Fig. 2C and 3A). We thought of the possibility that there might be a mechanism that prevents the binding of Ime1 at the very early stages under sporulation conditions. For such a mechanism, the higher-order chromatin structure at the *IME2* promoter or the existence of some inhibitory factor on the promoter may be considered. The repressive chromatin structure during the mitotic growth condition is known to be maintained by the Rpd3-Sin3 HDAC complex, which is tethered to the URS1 site through the interaction between Sin3 and Ume6, a DNA-binding protein that binds to URS1. So we asked whether the chromatin structure at the *IME2* promoter and the expression of *IME2* would be altered in the absence of HDAC. Under vegetative growth conditions, the MNase digestion pattern between nt −20 and −330 of both the *rpd3*Δ and *sin3*Δ strains was notably different from that of the wild type; i.e., novel cutting bands appeared in this region, and the intensity of the ones corresponding to nt −20 and −180 was decreased (Fig. 5A, open triangles and asterisks). On the other hand, the digestion pattern between nt −330 and −620 in both deletion strains was similar to that of the wild type. This result suggests that, in the absence of the Rpd3-Sin3 complex, the −1 and −2

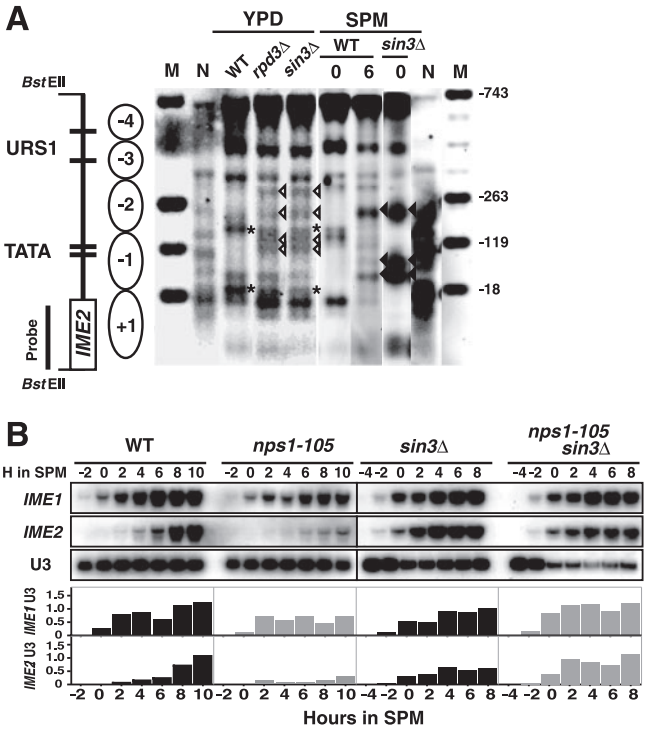

FIG. 5. Effects of *RPD3* and *SIN3* deletions on the chromatin structure and the expression of the *IME2* gene. (A) Nucleosome mapping by MNase digestion for the *rpd3*Δ (WHS20-D) and *sin3*Δ (WMY30-D) strains. Numbers indicate the time in hours (h) after the shift to SPM, and N denotes the naked DNA control. WT, wild type. Markers are as described in the legend to Fig. 1. (B) Northern blot analysis of *IME1* and *IME2* mRNA levels in the *sin3*Δ and *nps1-105 sin3*Δ cells. The strains used were wild type (W303-1D), *nps1-105* (WTH-1D), *sin3*Δ (WMY30-D), and *nps1-105 sin3*Δ (WMY31-D). RNA samples were hybridized with radioactively labeled *IME1* and *IME2* probes. The U3 small nuclear RNA probe was used as a loading control. These experiments were performed three times with good consistency. Typical results are presented.

nucleosomes might not be positioned in ordered array, whereas the −3 and −4 ones, which span URS1 sites, would be so positioned. The maintenance of the positioning of −3 and −4 nucleosomes in the absence of Rpd3-Sin3 complex is consistent with the finding of Goldmark et al. on the promoter of *REC104*, another URS1-containing gene (9). We assessed the level of *IME2* expression by using a reporter construct that expressed β-galactosidase from the *IME2* promoter (*IME2p*::*lacZ*) and detected 20-times-higher β-galactosidase activity in vegetatively growing *rpd3*Δ cells (12.46 ± 3.96 Miller units) than in the wild-type ones (0.57 ± 0.20 Miller units). However, the level of *IME2* derepression in *rpd3*Δ cells under mitotic conditions was five times lower than that of *ume6*Δ cells (66.7 ± 6.24 Miller units). These results are consistent with the previously described ones that were determined by Northern blot analysis (9), indicating that the role of the positioning of −1 and −2 nucleosomes for the repression of the *IME2* gene at mitosis might be partial.

Interestingly, on the other hand, a significant amount of *IME2* mRNA appeared in either the *sin3*Δ or *rpd3*Δ strain at the time of shifting the cells to SPM, where no *IME2* mRNA was detectable in the wild type (Fig. 5B). In the *sin3*Δ strain, the appearance and accumulation of *IME2* mRNA occurred almost concurrently with that of *IME1* mRNA; whereas in the wild-type strain, *IME2* mRNA appeared with a delay of approximately 4 to 6 h from the appearance of the *IME1* mRNA. The *ime1*Δ mutation strongly blocked the induction of *IME2* expression in the *rpd3*Δ strain, as reported earlier (4; data not shown). We also found that the MNase cutting pattern of the *IME2* promoter in *sin3*Δ and *rpd3*Δ strains at the time of the shift to SPM was similar to that of the wild type after a 6-h incubation in SPM, when the gene expression actively occurred (data for *rpd3*Δ strain not shown).

In the case of the *nps1-105 sin3*Δ or the *nps1-105 rpd3*Δ double mutant, the *IME2* mRNA appeared and accumulated with kinetics similar to that for the *sin3*Δ or *rpd3*Δ single mutant, showing that RSC was dispensable when the chromatin structure of −1 and −2 nucleosomes was abrogated in the absence of HDAC (Fig. 5B, data for the *nps1-105 rpd3*Δ strain not shown).

Rpd3-Sin3 complex is continuously present at URS1 regardless of the transcriptional condition of *IME2*. As described in the previous section, in the absence of HDAC, the chromatin structure at nucleosomes −1 and −2 of the *IME2* promoter was abrogated; and *IME2* transcription occurred with earlier timing. If the chromatin structure at the TATA box of *IME2* promoter prevents the binding of Ime1 at the very early stages of meiosis, this chromatin structure should be remodeled by RSC before the binding of Ime1. However, this was not the case, because the recruitment of RSC to TATA depended on Ime1 (Fig. 4A). Therefore, we considered the possibility that the Rpd3-Sin3 complex itself or a factor(s) associated with the complex might have blocked the binding of Ime1 to prevent transcription at the very early stages of meiosis. If so, Rpd3-Sin3 complex would be expected to be present at the URS1 site at this stage of meiosis. To examine this issue, we carried out ChIP analysis with anti-Rpd3 and found that Rpd3 was present at the *IME2*-URS1 site at all time points tested (Fig. 6). The amount of URS1 DNA coimmunoprecipitated with Rpd3 was rather higher when the cells were in the meiotic condition than in the vegetative growth one. A similar result was obtained for *SPO13*, another gene carrying the URS1 site. These results demonstrate that the Rpd3-Sin3 complex continuously bound URS1 and suggest a possibility that the Rpd3-Sin3 complex itself or some unidentified factor(s) that associates with the complex might contribute to the prevention of *IME2* expression at the very early stages of meiosis.

DISCUSSION

Our report presents the first evidence that the TATA box of the *IME2* gene, one of the key regulators of meiosis, is occupied by precisely positioned nucleosomes when the gene is in the repressed condition and that this nucleosome positioning is altered by RSC, which is recruited to the promoter by Ime1, to allow gene expression when the cells enter the meiotic condition. Our study also showed that the presence of the Rpd3-Sin3 complex at the *IME2* promoter plays an important role not only in maintaining the repressive chromatin structure at mitosis but also for ensuring the proper timing of the *IME2* expression in meiosis. Based on our results, we propose a model for the transcriptional regulation of *IME2* in the context

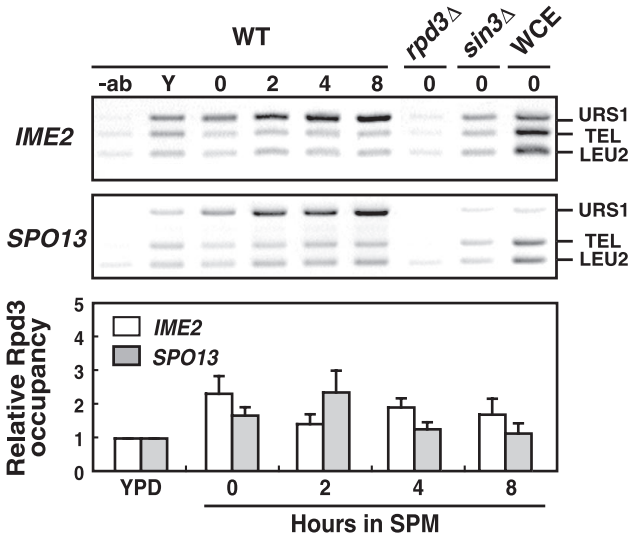

FIG. 6. The Rpd3-Sin3 complex is continuously present at the URS1 site. Wild-type (WT; W303-1D) and *nps1-105* (WTH-1D) cells were processed for ChIP analysis with anti-Rpd3 antibody (-ab). Y denotes a sample from cells vegetatively growing in YPD medium, and numbers indicate the time in hours after the shift to SPM. Typical results are presented in the upper two panels. The average amount of immunoprecipitated DNA obtained from five independent experiments was calculated and processed as described in the legend to Fig. 2B and is shown as a bar graph at the bottom.

of chromatin, in which the activation of the gene is achieved by a three-step process (Fig. 7). As the first step, histone H3 acetylation at URS1 takes place when the cells are in a medium containing acetate as the sole carbon source. When the cells are starved for nitrogen (SPM), as the second step, Ime1 is induced and activated by phosphorylation; however, the binding of Ime1 to URS1 is prevented by an unknown mechanism. Then, as the last step, Ime1 overcomes this inhibition, binds URS1, and recruits RSC to remodel the nucleosome that occupies the TATA sequence. The binding of Ime1 to URS1 is considered to be the rate-limiting step of this process. Previous genetic studies suggested that Ime1 plays two roles at the onset of *IME2* expression: (i) relieving Sin3 repression and (ii) providing an activator domain to Ume6 (37). Our study revealed that the former function of Ime1 involves the recruitment of RSC to untie the repressive chromatin structure at the TATA box, not the elimination or the inhibition of HDAC to induce the histone acetylation at URS1.

Our study showed that the molecular basis of *IME2* activation is much more complicated than was thought previously, and our results prompt several novel questions, which we discuss below.

What is the role of Gcn5/HAT and histone H3 acetylation in *IME2* expression? In the absence of Gcn5, Ime1 did not stably bind to URS1 (Fig. 3C). Although Gcn5 was shown to be responsible for the hyperacetylation of histone H3 at URS1

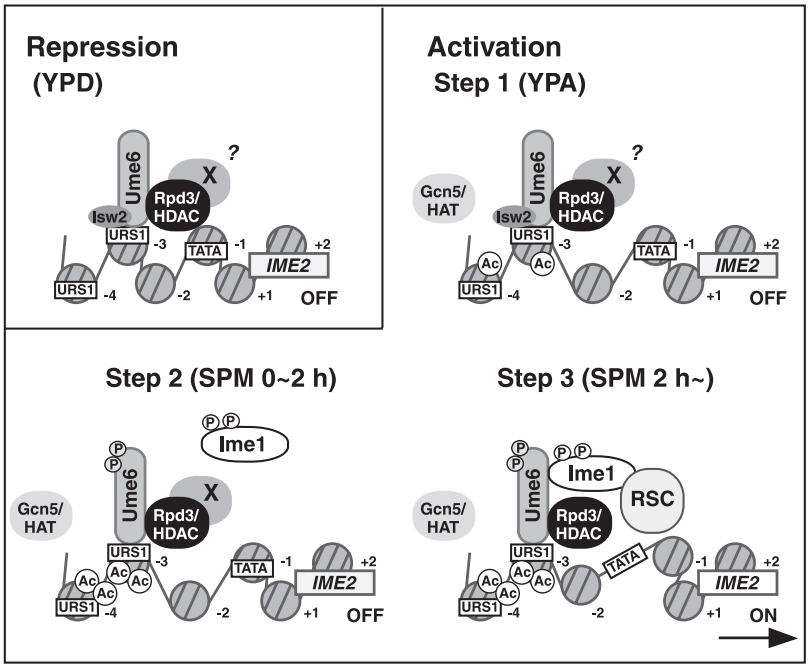

FIG. 7. A model for the transcriptional regulation of *IME2* by chromatin remodelers and Ime1. When the cells are vegetatively growing in rich medium containing either glucose or acetate as the sole carbon source (YPD and YPA), four nucleosomes indicated as −1 to −4 are positioned at the promoter of *IME2* in an ordered array where nucleosome −1 masks the two TATA sequences. The proper positioning of −1 and −2 nucleosomes is fully dependent on the Rpd3-Sin3 complex, and the gene expression is completely repressed. When acetate is the sole carbon source (YPA), a gradual increase in the histone H3 acetylation at nucleosomes −3 and −4 takes place. The acetylated state of nucleosomes −3 and −4 might affect the higher-order chromatin structure, but does not alter the positioning of nucleosomes in the ordered array, and the gene is still in the repressed condition. When the cells are transferred to SPM, Ime1 expression is accelerated and activated by phosphorylation. However, at the very early stages in SPM (0 to ~2 h), the binding of Ime1 is prevented by some unidentified factor(s) (X) in a manner dependent on the Rpd3-Sin3 complex. Then, Ime1 binds to Ume6 and, in turn, recruits RSC, and the remodeling of nucleosomes −1 and −2 by RSC occurs to allow gene expression.

(Fig. 2B), unexpectedly, the kinetics of the H3 acetylation did not coincide with that of the binding of Ime1 to URS1: i.e., the acetylation level of H3 increased long before the expression of Ime1, and it decreased after a 4-h incubation in SPM, when a large amount of Ime1 binding was obvious (Fig. 2C and 3A). Ime1 is tethered to URS1 by binding to Ume6 (28), and neither binding activity for histones nor the presence of a domain that binds acetylated lysine has so far been detected in Ime1. Considering the results that hyperacetylation of H3 at URS1 itself did not affect the positioning of nucleosomes at the *IME2* promoter (Fig. 1) and the RSC complex, which contains multiple bromodomain proteins known to directly bind acetylated lysine, did not bind to URS1 (Fig. 3B), this modification might affect the higher-order chromatin structure by changing the internucleosomal interaction to help the efficient binding of Ime1 (Fig. 7, step 1). In addition, our results suggest a possibility that Gcn5 plays an additional role, independent of histone H3 acetylation, for the stable binding of Ime1.

What mechanism makes a delay in the Ime1 binding to URS1? Our study suggested a possibility that the Rpd3-Sin3 complex itself or a factor(s) associated with the complex blocked the binding of Ime1 at the very early stages of meiosis. One of the possible candidates for this factor is the Set3 complex, because the expression of *IME2* in *set3*Δ cells was reported to occur earlier than in the wild-type ones (20). In addition, Cpr1, a component of the Set3 complex, was shown to physically interact with the Rpd3-Sin3 complex (1). Another candidate is Hac1 ($Hac1^i$). *HAC1* mRNA is spliced in response to the accumulation of unfolded proteins in the endoplasmic reticulum, and only this form is translated (see reference 30 and references therein). When nitrogen is present at high concentrations, *HAC1* mRNA is spliced; and its product, $Hac1^i$, physically interacts with Rpd3-Sin3 complex to repress the EMG transcription (30, 31). So we monitored the kinetics of *IME2* expression under meiotic conditions in *set3*Δ and *hac1*Δ homodiploids by using an *IME2p*::*lacZ* reporter construct and verified that the reporter gene expression occurred with earlier timing in the *hac1*Δ strain than in the wild type (Inai et al., unpublished result). In the case of *set3*Δ, although we detected little difference in the expression level of *IME2p*::*lacZ* between it and the wild type, deletion of the gene on the *hac1*Δ background enhanced the reporter gene expression. However, in both the *hac1*Δ and *hac1*Δ *set3*Δ strains, the acceleration of the *IME2p*::*lacZ* expression was only partial compared with that in the *rpd3*Δ strain (β-galactosidase activities in the wild type, *rpd3*Δ, *hac1*Δ, and *set3*Δ *hac1*Δ cells at 4 h in SPM of 26.1 ± 9.6, 314.7 ± 66.6, 53.9 ± 11.1, and 161 ± 18.2 Miller units, respectively) (Inai et al., unpublished result). Therefore, we consider that, in addition to $Hac1^i$ and the Set3 complex, there may still be an unidentified factor(s) that associates with the Rpd3-Sin3 complex and makes a delay in Ime1 binding at the very early stages of meiosis. Alternatively, the Rpd3-Sin3 complex itself, with the help of $Hac1^i$ and the Set3 complex, may play a role in this retardation. In either case, questions as to when this repressive structure for Ime1 binding is formed around the Rpd3-Sin3 complex and how this repressive condition is resolved remain enigmatic.

In contrast to our results, Pnueli et al. reported that the Rpd3-Sin3 complex is transiently removed from the URS1 site and replaced with Ime1 shortly after the shift to SPM (21). Earlier coimmunoprecipitation experiments, however, showed that the HDAC is associated with Ume6 under meiotic conditions (17). In addition, recent studies showed that Ume6 is a stable component of the Rpd3-Sin3 complex termed Rpd3L (6, 7). In our ChIP experiment, the anti-Rpd3 antibody efficiently coimmunoprecipitated *IME2*- and *SPO13*-URS1 sequences even when the H3 acetylation level had reached its highest, 2 h after the shift to SPM (Fig. 2 and 6). We repeated this ChIP analysis with anti-Rpd3 antibody five times each for *IME2*- and *SPO13*-URS1 and obtained highly reproducible results. The reason for this discrepancy between Pnueli's result and ours is unknown. The major difference in the experimental conditions, in addition to the difference in strain backgrounds, is that Pneuli's group analyzed Rpd3 binding to the *IME2* promoter by using the cells carrying *IME2* on a high-copy-number vector, whereas we analyzed it on the genomic locus. There are a number of genes in yeast that require the Rpd3-Sin3 complex for repression and/or activation independently of Ume6 (2, 25, 26). Because a significant number of metabolic genes are transiently repressed at the early stage of meiosis (22), it is possible that the binding of the Rpd3-Sin3 complex to *IME2*-URS1 on a high-copy plasmid would decrease if the complex is required at a large number of loci at this stage.

What is the biological role for delaying the expression of *IME2* from that of *IME1*? One possible answer to this question is that this delay might ensure the accumulation of a sufficient amount of *IME1* mRNA and then, as a result, that of *IME2* mRNA. The *IME1* expression is negatively regulated by *IME2* in two ways. First, the expression of Ime2 leads to the eventual repression of *IME1* transcription (31, 32); second, Ime2 phosphorylates Ime1 to target it for degradation (10). In the wild-type cells, the amounts of *IME1* and *IME2* mRNA reached values 1.3 times and 1.1 times higher than those of the control U3 RNA by 8-h and 10-h incubations in SPM, respectively (Fig. 5B). On the other hand, in the case of the *sin3*Δ cells, the maximal amounts of *IME1* and *IME2* mRNA were 90% and 60%, respectively, of the U3 RNA during the 8-h incubation in SPM. These results indicate that the expression of *IME2* with early timing affected the levels of both *IME1* and *IME2* transcripts. Precise induction of defined sets of genes at specific stages of differentiation is particularly important for eukaryotes. The regulation of transcriptional activation involving the control of timing described here might also be functioning in higher eukaryotes.

ACKNOWLEDGMENTS

This work was supported in part by grants-in-aid (no. 11239207 and 16026299) for scientific research from the Ministry of Education, Science, Sports and Culture of Japan.

REFERENCES

1. **Arévalo-Rodriguez, M., M. E. Cardenas, X. Wu, S. D. Hanes, and J. Heitman.** 2000. Cyclophilin A and Ess1 interact with and regulate silencing by the Sin3-Rpd3 histone deacetylase. EMBO J. **19:**3739–3749.
2. **Bernstein, B. E., J. K. Tong, and S. L. Schreiber.** 2000. Genome wide studies of histone deacetylase function in yeast. Proc. Natl. Acad. Sci. USA **97:** 13708–13713.
3. **Boeger, H., J. Griesenbeck, J. S. Strattan, and R. D. Kornberg.** 2003. Nucleosomes unfold completely at a transcriptionally active promoter. Mol. Cell **11:**1587–1598.
4. **Bowdish, K. S., and A. P. Mitchell.** 1993. Bipartite structure of an early meiotic upstream activation sequence from *Saccharomyces cerevisiae*. Mol. Cell. Biol. **13:**2172–2181.

5. **Burgess, S. M., M. Ajimura, and N. Kleckner.** 1999. GCN5-dependent histone H3 acetylation and RPD3-dependent histone H4 deacetylation have distinct, opposing effects on *IME2* transcription, during meiosis and during vegetative growth, in budding yeast. Proc. Natl. Acad. Sci. USA **96:**6835–6840.
6. **Carrozza, M. J., L. Florens, S. K. Swanson, W. J. Shia, S. Anderson, J. Yates, M. P. Washburn, and J. L. Workman.** 2005. Stable incorporation of sequence specific repressors Ash1 and Ume6 into the Rpd3L complex. Biochim. Biophys. Acta **1731:**77–87.
7. **Carrozza, M. J., B. Li, L. Florens, T. Suganuma, S. K. Swanson, K. K. Lee, W. J. Shia, S. Anderson, J. Yates, M. P. Washburn, and J. L. Workman.** 2005. Histone H3 methylation by Set2 directs deacetylation of coding regions by Rpd3S to suppress spurious intragenic transcription. Cell **123:**581–592.
8. **Chu, S., J. DeRisi, M. Eisen, J. Mulholland, D. Botstein, P. O. Brown, and I. Herskowitz.** 1998. The transcriptional program of sporulation in budding yeast. Science **282:**699–705.
9. **Goldmark, J. P., T. G. Fazzio, P. W. Estep, G. M. Church, and T. Tsukiyama.** 2000. The Isw2 chromatin remodeling complex represses early meiotic genes upon recruitment by Ume6p. Cell **103:**423–433.
10. **Guttmann-Raviv, N., S. Martin, and Y. Kassir.** 2002. Ime2, a meiosis-specific kinase in yeast, is required for destabilization of its transcriptional activator, Ime1. Mol. Cell. Biol. **22:**2047–2056.
11. **Hecht, A., S. Strahl-Bolsinger, and M. Grunstein.** 1999. Mapping DNA interaction sites of chromosomal proteins. Cross linking studies in yeast. Methods Mol. Biol. **119:**469–479.
12. **Honigberg, S. M., and K. Purnapatre.** 2003. Signal pathway integration in the switch from the mitotic cell cycle to meiosis in yeast. J. Cell Sci. **116:** 2137–2147.
13. **Kadosh, D., and K. Struhl.** 1997. Repression by Ume6 involves recruitment of a complex containing Sin3 corepressor and Rpd3 hstone deacetylase to target promoters. Cell **89:**365–371.
14. **Kasten, M. M., S. Dorland, and D. J. Stillman.** 1997. A large protein complex containing the yeast Sin3p and Rpd3p transcriptional regulators. Mol. Cell. Biol. **17:**4852–4858.
15. **Koyama, H., M. Itoh, K. Miyahara, and E. Tsuchiya.** 2002. Abundance of the RSC nucleosome-remodeling complex is important for the cells to tolerate DNA damage in *Saccharomyces cerevisiae*. FEBS Lett. **531:**215–221.
16. **Koyama, H., T. Nagao, T. Inai, K. Miyahara, Y. Hayashida, K. Shirahige, and E. Tsuchiya.** 2004. RSC nucleosome-remodeling complex plays prominent roles in transcriptional regulation throughout budding yeast gametogenesis. Biosci. Biotechnol. Biochem. **68:**909–919.
17. **Lamb, T. M., and A. P. Mitchell.** 2001. Coupling of *Saccharomyces cerevisiae* early meiotic gene expression to DNA replication depends upon *RPD3* and *SIN3*. Genetics **157:**545–556.
18. **Mitchell, A. P.** 1994. Control of meiotic gene expression in *Saccharomyces cerevisiae*. Microbiol. Rev. **58:**56–70.
19. **Ng, H. H., F. Robert, R. A. Young, and K. Struhl.** 2002. Genome-wide location and regulated recruitment of the RSC nucleosome-remodeling complex. Genes Dev. **16:**806–819.
20. **Pijnappel, W. W. M. P., D. Schaft, A. Roguev, A. Shevchenko, H. Tekotte, M. Wilm, G. Rigaut, B. Seraphin, R. Aasland, and A. F. Stewart.** 2001. The *S. cerevisiae* SET3 complex includes two histone deacetylases, Hos2 and Hst1, and is a meiotic-specific repressor of the sporulation gene program. Genes Dev. **15:**2991–3004.
21. **Pnueli, L., I. Edry, M. Cohen, and Y. Kassir.** 2004. Glucose and nitrogen regulate the switch from histone deacetylation to acetylation for expression of early meiosis-specific genes in budding yeast. Mol. Cell. Biol. **24:**5197–5208.
22. **Primig, M., R. M. Williams, E. A. Winzeler, G. G. Tevzadze, A. R. Conway, S. Y. Hwang, R. W. Davis, and R. E. Esposito.** 2000. The core meiotic transcriptome in budding yeasts. Nat. Genet. **26:**415–423.
23. **Reinke, H., and W. Horz.** 2003. Histones are first hyperacetylated and then lose contact with the activated *PHO5* promoter. Mol. Cell **11:**1599–1607.
24. **Rigaut, G., A. Shevchenko, B. Rutz, M. Wilm, M. Mann, and B. Seraphin.** 1999. A generic protein purification method for protein complex characterization and proteome exploration. Nat. Biotechnol. **17:**1030–1032.
25. **Robert, F., D. K. Pokholok, N. M. Hannett, N. J. Rinaldi, M. Chandy, A. Rolfe, J. L. Workman, D. K. Gifford, and R. A. Young.** 2004. Global position and recruitment of HATs and HDACs in the yeast genome. Mol. Cell **16:**199–209.
26. **Robyr, D., Y. Suka, I. Xenarios, S. K. Kurdistani, A. Wang, N. Suka, and M. Grunstein.** 2002. Microarray deacetylation maps determine genome-wide functions for yeast histone deacetylases, Cell **17:**437–446.

26a. **Rothstein, R.** 1983. One-step gene disruption in yeast. Methods Enzymol. **101:**202–211.

27. **Rothstein, R.** 1991. Targeting, disruption, replacement, and allele rescue: integrative DNA transformation in yeast. Methods Enzymol. **194:**281–301.
28. **Rubin-Bejerano, I., S. Mandel, K. Robzyk, and Y. Kassir.** 1996. Induction of meiosis in *Saccharomyces cerevisiae* depends on conversion of the transcriptional repressor Ume6 to a positive regulator by its regulated association with the transcriptional activator Ime1. Mol. Cell. Biol. **16:**2518–2526.
29. **Rundlett, S. E., A. A. Carmen, N. Suka, B. M. Turner, and M. Grunstein.** 1998. Transcriptional repression by *UME6* involves deacetylation of lysine 5 of histone H4 by *RPD3*. Nature **392:**831–835.
30. **Schröder, M., J. S. Chang, and R. J. Kaufman.** 2000. The unfolded protein response represses nitrogen-starvation induced developmental differentiation in yeast. Genes Dev. **14:**2962–2975.
31. **Schröder, M., R. Clark, C. Y. Liu, and R. J. Kaufman.** 2004. The unfolded protein response represses differentiation through the RPD3-SIN3 histone deacetylase. EMBO J. **23:**2281–2292.
32. **Shefer-Vaida, M., A. Sherman, T. Ashkenazi, K. Robzyk, and Y. Kassir.** 1995. Positive and negative feedback loops affect the transcription of *IME1*, a positive regulator of meiosis in *Saccharomyces cerevisiae*. Dev. Genet. **16:**219–228.
33. **Smith, C. L., R. Horowitz-Scherer, J. F. Flanagan, C. L. Woodcock, and C. L. Peterson.** 2003. Structural analysis of the yeast SWI/SNF chromatin remodeling complex. Nat. Struct. Biol. **10:**141–145.
34. Reference deleted.
35. **Tsuchiya, E., T. Hosotani, and T. Miyakawa.** 1998. A mutation in *NPS1*/*STH1*, an essential gene encoding a component of a novel chromatin-remodeling comlex RSC, alters the chromatin structure of *Saccharomyces cerevisiae* centromeres. Nucleic Acids Res. **26:**3286–3292.
36. **Vershon, A. K., and M. Pierce.** 2000. Transcriptional regulation of meiosis in yeast. Curr. Opin. Cell Biol. **12:**334–339.
37. **Washburn, B. K., and R. E. Esposito.** 2001. Identification of the Sin3-binding site in Ume6 defines a two-step process for conversion of Ume6 from a transcriptional repressor to an activator in yeast. Mol. Cell. Biol. **21:**2057–2069.
38. **Xiao, Y., and A. P. Mitchell.** 2000. Shared roles of yeast glycogen synthase kinase 3 family members in nitrogen-responsive phosphorylation of meiotic regulator Ume6p. Mol. Cell. Biol. **20:**5447–5453.
39. **Yukawa, M., S. Katoh, T. Miyakawa, and E. Tsuchiya.** 1999. Nps1/Sth1, a component of an essential chromatin-remodeling complex of *Saccharomyces cerevisiae*, is required for the maximal expression of early meiotic genes. Genes Cells **4:**99–110.
40. **Yukawa, M., H. Koyama, K. Miyahara, and E. Tsuchiya.** 2002. Functional differences between *RSC1* and *RSC2*, components of a growth essential chromatin-remodeling complex of *Saccharomyces cerevisiae*, during the sporulation process. FEMS Yeast Res. **2:**87–91.